

Preroughening, fractional-layer occupancies, and phase separation at a disordered flat metal surface

Santi Prestipino*

Istituto Nazionale per la Fisica della Materia and International School for Advanced Studies, via Beirut 2-4, 34013 Trieste, Italy

Erio Tosatti[†]

*Istituto Nazionale per la Fisica della Materia and International School for Advanced Studies, via Beirut 2-4, 34013 Trieste, Italy
and International Centre for Theoretical Physics, Trieste, Italy*

(Received 5 September 1997; revised manuscript received 8 December 1997)

We study the phase separation that a particle-conserving (“canonical”) full-layered metal surface must undergo at temperatures between preroughening and roughening. The separation is into two disordered flat (DOF) domains of opposite order parameter with a step between them, each domain exhibiting a half-filled top layer. It is shown that both Gibbs-ensemble simulation and canonical Monte Carlo plus finite-size scaling, carried out on a specific lattice Hamiltonian model, demonstrate this phase-separation phenomenon microscopically. A number of existing particle-conserving molecular-dynamics simulations for fcc(110) metal surfaces are then analyzed, and it is found that some display clear, previously unnoticed evidence of this DOF phase separation. Its main signal is a plateau of layer occupancies with temperature, around values close to $\frac{3}{4}$ for the first surface layer, and around $\frac{1}{4}$ for the adatom layer. It is proposed that this unusual type of phase separation could be observable on sufficiently step-free metal surfaces. [S0163-1829(98)07215-4]

I. INTRODUCTION

Recently, there has been growing interest in the thermal disordering of crystal surfaces since the introduction, by den Nijs and Rommelse, of the preroughening transition leading to *disordered flat* phases,¹ and the suggestion that they should be realized on metal surfaces.²⁻⁴ Preroughening (PR) is an equilibrium phase transition at $T=T_{PR}$ between the ordered flat (OF) phase and the disordered flat (DOF) phase. Conventional roughening occurs at a higher temperature $T_R>T_{PR}$. As recent studies have brought out, the ultimate mechanism leading to PR is an *extended repulsive* interaction between parallel steps, favoring the onset of a disordered array of alternating up and down steps. Repulsive interactions between parallel steps originate, for example, from the elastic strains accompanying the steps.⁵ PR is expected to be present so long as parallel steps repel each other strongly enough, if at the same time antiparallel steps do not.

Surface reconstruction, found at $T=0$ in many metal surfaces, provides another route to PR. Within solid-on-solid (SOS) models, a reconstructed ground state can be obtained, for example, when the first-neighbor height-height interaction is negative, and only second- and further-neighbor interactions are positive. Most of the existing studies focus on the (110) face of noble metals, with a tendency, either manifest or latent, toward (1×2) missing-row reconstruction. SOS models have been used to address this case in Refs. 6, 7, 2, and 8. In particular, thermal deconstruction of (1×2) surfaces, e.g., Au(110), is believed to lead to a stable DOF phase below roughening.^{2,8} So far, on the other hand, no clear evidence of PR has been reported for *unreconstructed*, i.e., (1×1) metal surfaces, like Ag, Cu, and Ni(110). Various SOS models predict the possibility of PR for these faces, at least under favorable conditions. Dormant reconstruction

tendencies^{2,8} as well as elastic parallel-step repulsion, are certainly present at these surfaces, but it is uncertain if they are strong enough. Therefore, to this date, it is not known to any quantitative level whether a real unreconstructed metal surface meets the conditions for a PR transition, and for a corresponding stable DOF phase below roughening. This situation clearly calls for a more intense experimental effort, as well as for realistic simulations.

A realistic simulation of PR on a metal surface is, in spite of the availability of reasonably good potentials and techniques, still a very difficult task, for two main reasons. The first are very tough requirements of large sizes and size scaling, as well as of very long simulation times. These requirements are mandatory for PR—a two-dimensional (2D) critical phenomenon—and even more so for surface roughening. The second, subtler reason, is the necessity to address PR within a grand-canonical ensemble, as clearly suggested by the jump from integer or nearly integer population of the top layer, to the half-integer population which characterizes the DOF phase. This requirement raises a difficulty, in particular for molecular dynamics (MD), where grand-canonical schemes are still under debate, and far from well established. What is available so far is a number of very reliable, good quality *canonical* (i.e., particle-conserving) MD simulations of metal surfaces, covering the relevant temperature range $T\approx T_R$.

Similar to simulation, experimental realization of a DOF phase on a metal surface also requires grand-canonical conditions, i.e., an adjustable particle number. Experimentally, grand-canonical conditions, despite the absence of evaporation and/or condensation which is a typical condition of study of metals under ultrahigh-vacuum conditions, are usually obtained by diffusion of adatoms to and from steps. At sufficiently high temperature, these diffusion processes will

generally be present, and make a metal surface effectively grand canonical, in a relatively slow experiment and in the presence of preexisting steps, inevitable in a real surface. Alternatively, approximate canonical conditions could be realized, for a limited time duration, in the center of a large flat surface terrace, for a surface of very good quality (low step concentration).

The question we pose here is the following: how would surface PR, and the subsequent onset of a DOF phase, manifest itself in such a fast, canonical experiment on a good quality metal surface, where particles do not have a chance to evaporate, and do not have the time to diffuse away to a step? Equivalently, how will PR show up in a realistic, particle-conserving MD or Monte Carlo (MC) simulation, unable by construction to change number of atoms, and thus to switch from a full to a half-full surface layer?

In the rest of this paper, we employ a lattice model of fcc(111) surfaces⁴ for a MC study of layer abundancies and occupancies (defined in Sec. II) at a fixed particle number. A possible phase separation into two DOF domains is introduced and its signature in terms of occupancies is presented. In Sec. III we demonstrate phase separation through a Gibbs-ensemble simulation of the lattice model. This calculation is followed in Sec. IV by the finite-size scaling analysis of layer occupancies under canonical conditions. Again, results indicate that the expected phase separation actually takes place. Based on this outcome, we review, in Sec. V, the results of realistic published MD simulations for several metal surfaces, and identify, for some of them, previously undetected signals of DOF phase separation. This finding is important, in that it invalidates many of the conclusions previously drawn by ignoring phase separation. Finally, it is suggested that the search of this phenomenon could and should be pursued experimentally.

II. LAYER OCCUPANCIES, ABUNDANCES, AND FINITE-SIZE BEHAVIOR

In a SOS model, a height variable is assigned at each site of a regular lattice so as to mark the border between the interior of the crystal (assumed to have no vacancies) and the outside. It is generally believed that SOS lattice models of crystal surfaces provide an acceptable (although rather qualitative) description of the surface thermodynamics in the area of roughening and growth. Recently, we have constructed a restricted SOS model for fcc(111) surfaces (called FCSOS) which exhibits, in a range of parameters, a PR transition at some $T=T_{\text{PR}}$.⁴ Above T_{PR} , there is a well-defined DOF phase characterized by a nonzero DOF order parameter, followed at a higher temperature T_R , by a roughening transition.

In the FCSOS model, the height-height interactions are all positive (nonreconstructive), but long ranged enough to give rise to a DOF phase with a half-occupied top layer and, consequently, a half-integer average height. The model is defined as follows: (a) heights are defined on a triangular lattice (three sublattices $l=0,1,2$); (b) a height $h_i=l \pmod{3}$ is required for any site i in sublattice l , so as to reproduce the typical $ABCABC\dots$ stacking of triangular planes in a fcc crystal; and (c) nearest-neighbor heights can only differ by $\Delta h^{(1)}=\pm 1, \pm 2$. The FCSOS Hamiltonian reads

$$H=J\sum_{(2)}\delta(|h_i-h_j|-3)+K\sum_{(3)}\delta(|h_i-h_j|-4) \\ +L\sum_{(4)}\delta(|h_i-h_j|-4), \quad (1)$$

where $\Sigma_{(n)}$ is a shorthand notation for the sum over all pairs of n th neighbors in the triangular lattice and couplings J , K , and L are taken positive, so as to have a finite step energy and to penalize parallel steps when approaching each other.

The minimal requirement to obtain a stable DOF phase in the FCSOS model is a nonzero L value.¹⁶ For $L=0$ there is no PR or DOF phase. This indicates that the longer-range part of the step-step repulsion is crucial in leading to a PR transition in the model. The hypothetical inclusion of longer-ranged, realistic power-law step-step repulsive interactions, even if not feasible at present, could be expected to favor PR even further. The phase diagram of the FCSOS model was worked out for $L=K$ in Ref. 4. In that case, the boundaries of the DOF region were found to be $e^{\beta J}\approx 1.5$ and $e^{\beta K}\approx 1.8$, with $\beta^{-1}=k_B T$.

Now, consider a SOS model of the crystal surface chosen in such a way as to exhibit a PR transition at $T=T_{\text{PR}}$. We force this surface (i.e., the whole semi-infinite crystal) to possess a fixed number of particles and thus a fixed average height $\bar{h}=(1/N_t)\sum_i h_i$ (h_i is the height at site i , and N_t is the number of sites in the plane). At a temperature T above T_{PR} , this system is in principle similar to an Ising model being brought below T_c , while keeping a fixed magnetization M . One expects in that case a phase separation into spin up and spin down domains, divided by a 1D interface. The up and down domain areas are in a ratio which is directly dictated by the required magnetization M . For the canonical surface above T_{PR} , it is natural to expect¹ a similar phase separation between even and odd parity (“even on top” and “odd on top”) DOF regions, separated by a monatomic step. Since the top layer is half-occupied within each DOF region, the phase-separated surface with canonically fixed “magnetization” M ($M=0$ corresponding to two equal-size regions, $M=\pm 1$ to a pure DOF phase) will generally exhibit fractional average lattice occupancies over a number of layers. Since phase separation is a macroscopic phenomenon, the corrections due to the monatomic step are negligible in the thermodynamic limit, and the occupancies will be determined by M only. More generally, dealing with SOS models, we can introduce a layer-dependent *abundance* a_n , besides the corresponding layer-dependent *occupancy* o_n . The n th layer abundance can be defined as

$$a_n=\frac{1}{\nu N_s}\sum_i \delta_{h_i,n}, \quad (2)$$

where ν is the number of sublattices [$\nu=2$ for fcc(110), and $\nu=3$ for fcc(111)] and N_s is the total number of sites in each sublattice (thus $\nu N_s=N_t$); a_n represents the probability to find the surface at layer n . A sum rule holds separately for each sublattice,

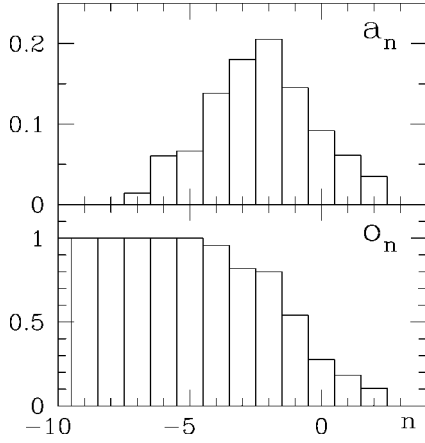


FIG. 1. Layer abundance and occupancy profiles for a crystal surface (schematic).

$$\sum_{k=-\infty}^{+\infty} a_{l+\nu k} = 1/\nu \quad (l=0, \dots, \nu-1), \quad (3)$$

reflecting the absence, in SOS models, of overhangs, and of totally surrounded inner-layer vacancies. The occupancy of layer n is determined by the abundances of all lower (or upper) ‘‘companion’’ layers m [i.e., those with $\text{mod}(n-m, \nu)=0$],

$$o_n = 1 - \nu \sum_{k=1}^{+\infty} a_{n-\nu k} = \nu \sum_{k=0}^{+\infty} a_{n+\nu k}. \quad (4)$$

A schematic illustration of surface abundances and occupancies is given in Fig. 1. For instance, a DOF surface in the FCSOS model spreads over four layers, with abundances close to $a_{-3}=0$, $a_{-2}=\frac{1}{6}$, $a_{-1}=\frac{1}{3}$, $a_0=\frac{1}{3}$, $a_1=\frac{1}{6}$, and $a_2=0$, and corresponding occupancies $o_{-3}=1$, $o_{-2}=1$, $o_{-1}=1$, $o_0=1$, $o_1=\frac{1}{2}$, and $o_2=0$.

Two phase-separated DOF domains, giving an overall magnetization M , will correspond to average abundances

$$a_n = \frac{1+M}{2} a_n^{(1)} + \frac{1-M}{2} a_n^{(2)}. \quad (5)$$

Conversely, the magnetization M is given in terms of $\bar{h} = \sum_n n a_n$ by

$$M = \frac{2\bar{h} - \bar{h}^{(1)} - \bar{h}^{(2)}}{\bar{h}^{(1)} - \bar{h}^{(2)}}. \quad (6)$$

For example, a FCSOS surface with an integer number of layers, corresponding to $M=0$, would give rise to two equal-size phase-separated domains, implying overall abundances $a_{-3}=0$, $a_{-2}=\frac{1}{12}$, $a_{-1}=\frac{1}{4}$, $a_0=\frac{1}{3}$, $a_1=\frac{1}{4}$, $a_2=\frac{1}{12}$, and $a_3=0$, and layer occupancies $o_{-3}=1$, $o_{-2}=1$, $o_{-1}=1$, $o_0=1$, $o_1=\frac{3}{4}$, $o_2=\frac{1}{4}$, and $o_3=0$. More generally, the phase-separated occupancies o_n for outermost crystal layers $n=-1, 0, 1, 2$, and 3 will be given, above T_{PR} , by $o_{-1}=1$, $o_0=1$, $o_1=(3+M)/4$, $o_2=(1+M)/4$, and $o_3=0$. This result is clearly not specific to the model just assumed. For example, phase separation can be easily seen to lead to

analogous occupancies in a rectangular surface for arbitrary M , in spite of the different symmetry and sublattice number.

Later in this paper, we shall seek a DOF-induced phase separation by means of numerical finite-size scaling. As a preliminary to that, we first consider the expected behavior, based on the Ising analogy mentioned above.

Phase separation in a system of lateral size N introduces a boundary, from which the free energy density can be written in the general form (similar to that for, e.g., smooth vicinal surfaces⁹),

$$f(N) = f_\infty - \mu N^{-1} + \mathcal{O}(N^{-3}), \quad (7)$$

where f_∞ is the thermodynamic-limit free energy of either phase, and μ is the boundary or step-free energy per unit length (step line tension). In the vicinal-surface problem, what determines the N^{-1} form of the dominant size correction is the *smoothness* of the step-free face, which implies for the step a locally finite transverse extension and a nonzero free energy (if instead the face were rough, the step width would diverge, and the first correction would be of order N^{-2}). In the present problem, a well-defined monatomic step between the two phase-separated regions also implies that global abundances (and occupancies) must differ from their macroscopic value (4) by corrections which are also of order N^{-1} , namely

$$a_n(N) = a_n^\infty + C_n N^{-1} + \mathcal{O}(N^{-3}), \quad (8)$$

where C_n should again be proportional to the step line tension μ . In analogy with the Ising case, we expect μ to be finite so long as the DOF order parameter is nonzero, and to vanish both at T_{PR} and at T_R .⁸ After these preliminaries, we can move on to consider the phase separation issue in a solvable Hamiltonian model.

III. DOF PHASE-SEPARATION: GIBBS-ENSEMBLE STUDY OF A LATTICE MODEL

Phase coexistence is the signature of a first-order transition with an abrupt change of at least one extensive quantity. The description of phase equilibria in fluids and fluid mixtures is a long-standing problem in the realm of computer simulation. Before the advent of the Gibbs-ensemble technique, the standard way to study phase separation was to calculate the chemical potential or the free energy of each phase during a long series of MC or MD simulations.¹⁰ When the two phases are found to share the same temperature, pressure, and chemical potential they are in equilibrium. Obviously, this procedure is rather impractical and enormously time consuming. The Gibbs-ensemble method provides a more direct route to phase coexistence, which is accomplished in a single simulation.¹¹ Its main use has been for fluid-fluid equilibria, such as liquid-gas coexistence in a simple fluid, but it has also been applied to other systems¹² (a comprehensive list of applications is included in Ref. 13).

The Gibbs-ensemble method relies on a reasonable number of successful particle insertions. As such, the Gibbs-ensemble method can only be used to study equilibria involving phases that are not too dense. In fact, this is just the case of interest here, since in a half-occupied layer (like the

topmost one in a DOF surface) there is enough room for insertions.

In order to illustrate the method, we consider classical liquid-gas coexistence, which was the context where the Gibbs-ensemble method has originally appeared. Particles are distributed into two separate boxes, each with its own periodic boundary conditions. The total particle number and the total volume are conserved. Moreover, particles only interact with other particles in the same box. These rules define an ensemble of configurations, called the Gibbs ensemble, which is equivalent, in the thermodynamic limit, to the *canonical* ensemble, even in presence of phase separation.¹⁴ The reason for this is that the two ensemble partition functions differ for at most a surface term.

In a Gibbs-ensemble simulation, MC moves of three kinds are considered: (1) displacement of a particle within a box, (2) change of the volume of one box at the expenses of the other, and (3) exchange of a particle between the boxes. As usual, moves are accepted according to detailed balance. At a first-order transition, the advantage of this method over the standard canonical MC simulation is obvious: it removes the interface between the two coexisting phases without preventing the exchange of particles and volume between them. Gibbs-ensemble simulations of a fluid system at a temperature lower than critical lead, in fact, to liquid in one box and gas in the other, both densities being equal to the coexistence values at that temperature.

Moving to our problem, we wish to adapt this method to the SOS problem. The main use of the FCSOS model in the present context is simply to provide a case study for DOF phase separation. We simulate this model in the Gibbs ensemble by considering two separate $\sqrt{N_t} \times \sqrt{N_t}$ “boxes” that can exchange “particles” with each other, in such a way that detailed balance holds at any MC step. Such a simulation setup would allow phase separation to develop if thermodynamically necessary.

MC moves of two kinds are included: (1) displacement of a randomly selected particle from a lattice site to another (sufficiently close by) within the same box, and (2) exchange of a random particle between the two boxes. Note that there is no volume exchange here. This means that although the mean heights of the two boxes can fluctuate, volume fluctuations of each are totally suppressed.¹⁵ This raises no problem for all transitions in the lattice models addressed here, and must be contrasted with the case of the liquid-gas transition, where phase coexistence is not conceivable without the possibility of volume exchange between the two phases. For PR and the DOF-phase coexistence we are interested in, the lack of volume fluctuations is of no consequence and fully justified.

Although the total mean surface height is kept fixed during the simulation, within each box the system is free to adjust its own mean height. If we start the simulation from a full-layered, $\bar{h}=0$, surface ($M=0$ in magnetic language), with FCSOS parameters corresponding to a smooth (OF) surface, each box should separately end up in that phase. If, instead, parameters call for a DOF phase, the system should phase-separate into two DOF surfaces, one with $\bar{h}=\frac{1}{2}$ in one box and another with $\bar{h}=-\frac{1}{2}$ in the other.

This is indeed what happens, as illustrated in Table I. The

TABLE I. Unnormalized abundances, $a_n N_s$, in a 60×60 FC-SOS lattice at $K=L=+\infty$, $e^{\beta J}=1.1$ (above) and 1.8 (below), corresponding to a DOF phase and a smooth phase, respectively. For each crystal layer, the average population is reported after three million sweeps. Evidence of a DOF phase separation in the Gibbs-ensemble simulation is striking.

layer	Gibbs ensemble box 1	Gibbs ensemble box 2	grand canonical
-4	0.00	0.00	0.00
-3	1.13	0.00	1.30
-2	599.97	1.18	600.10
-1	1198.85	600.06	1198.72
0	1198.87	1198.81	1198.70
1	600.03	1198.82	599.90
2	1.15	599.94	1.28
3	0.00	1.19	0.00
4	0.00	0.00	0.00

layer	Gibbs ensemble box 1	Gibbs ensemble box 2	grand canonical
-3	0.00	0.00	0.00
-2	48.22	48.57	49.41
-1	1151.47	1151.74	1150.50
0	1200.00	1200.00	1199.99
1	1151.78	1151.43	1150.59
2	48.53	48.26	49.50
3	0.00	0.00	0.00

table shows the height statistics (i.e., unnormalized abundances) from a Gibbs-ensemble simulation of a double 60×60 lattice where, after equilibration, averages were computed over about 3 000 000 MC sweeps. At the higher temperature, the system clearly phase separates into a pair of DOF surfaces 1 ML apart. Comparison with an independent MC simulation carried out in the grand-canonical ensemble confirms (Table I) that both the OF and DOF phases become ensemble-insensitive in the thermodynamic limit. Moreover, we find that energy, specific heat, interface width, and order parameters are to a very good approximation the same for both ensembles (Table II).

Although the evidence provided by the Gibbs-ensemble simulation is striking, a more direct proof of the thermodynamical phase coexistence should still be provided. For this reason, we decided to calculate the chemical potential of the surface in each box, defined as the intensive parameter conjugate to the mean surface height. This quantity describes the response of the surface to the attempt of inserting one particle. Widom first derived in the context of simple fluids the relationship between the chemical potential and the insertion probability for an extra particle.¹⁷ In a canonical setup, namely, at fixed \bar{h} , one can readily show that an expression similar to that originally found by Widom holds for μ ,

$$\mu = -k_B T \ln \left\langle \frac{1}{N_t} \sum_{i=1}^{N_t} e^{-\beta \Delta E_i^+} \right\rangle, \quad (9)$$

where the average (over a canonical ensemble of surface configurations) is the SOS analog of the insertion probabil-

TABLE II. Equilibrium averages in a 60×60 FCSOS lattice at $K=L=+\infty$, $e^{\beta J}=1.1$ (above) and 1.8 (below), corresponding to a DOF phase and a smooth phase, respectively (see Ref. 13 for the precise definition of each quantity). The equilibrium properties are practically the same in the two ensembles (see Table I).

layer	Gibbs ensemble box 1	Gibbs ensemble box 2	grand canonical
u/J	0.471 188	0.471 082	0.470 938
δh^2	0.920 270	0.920 429	0.920 552
P	0.020 809	0.020 732	0.028 918
S	0.348 370	0.347 974	0.347 519
C_V	0.002 899	0.002 909	0.002 932
dC_V	-0.000 610	-0.000 616	-0.000 621
$\frac{dT}{dT}$			
χ_P	0.028 427	0.028 345	0.054 829
χ_S	0.073 759	0.073 664	0.133 141

layer	Gibbs ensemble box 1	Gibbs ensemble box 2	grand canonical
u/J	0.126 787	0.126 941	0.128 037
δh^2	0.747 144	0.747 200	0.748 738
P	0.838 741	0.838 629	0.835 172
S	0.816 233	0.816 390	0.812 806
C_V	0.247 216	0.248 825	0.251 141
dC_V	0.091 036	0.102 770	0.136 561
$\frac{dT}{dT}$			
χ_P	0.463 799	0.459 185	0.521 648
χ_S	0.609 640	0.603 688	0.759 530

ity, and ΔE_i^+ is the difference in energy between a surface with one more particle on site i and the original surface (see Appendix A).

Actually, as shown by Smit and Frenkel,¹⁸ formula (9) should be modified for application in the Gibbs ensemble. However, as shown in Appendix A, the lack of volume fluctuations in the present case leads to a simple extension of form (9),

$$\mu = -k_B T \ln \left\{ \frac{1}{2} \sum_{\alpha=1,2} \left\langle \frac{1}{N_i} \sum_{i=1}^{N_i} e^{-\beta \Delta E_i^+} \right\rangle \right\}. \quad (10)$$

In the Gibbs-ensemble simulation, the two boxes have in principle a finite probability to interchange their identity, even under phase-separation conditions. However, our sizes are sufficiently large that this switch does not occur within $3M$ sweeps. Because of this, the separate averages for each box can be used to define separate chemical potentials.

Even if \bar{h} 's are different we expect, due to the identical nature of the phases in the two boxes, that the quantity in Eq. (9) be the same for both. We take a double lattice of two different lateral sizes, 36 and 60, at $e^{\beta J}=1.1$ and $K=L=+\infty$. After a 3 000 000-sweep simulation, we find $\beta\mu(\text{box1})=1.8023(1)$ and $\beta\mu(\text{box2})=1.8022(2)$ for the double 36×36 lattice, and $\beta\mu(\text{box1})=1.80424(7)$ and $\beta\mu(\text{box2})=1.80438(4)$ for the double 60×60 lattice. Therefore, within the numerical errors, the two chemical potentials are the same. We conclude that Gibbs-ensemble MC

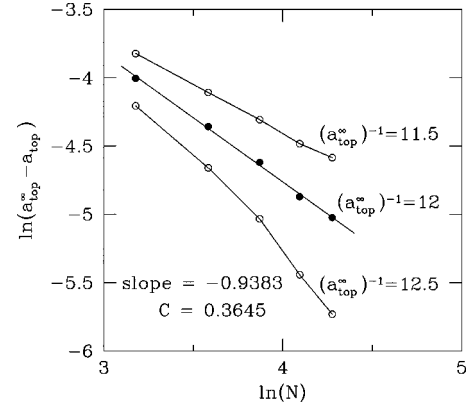


FIG. 2. Top layer (layer 1, adatoms) occupancy as a function of the inverse size for a FCSOS model with full layers. The best fit is with $a_{\text{top}}^{\infty} = \frac{1}{12}$ and an exponent near -1 , indicating phase separation into DOF domains.

clearly demonstrates the existence of the DOF phase separation, once the average surface height is clamped to a fixed value.

IV. SURFACE OCCUPANCIES AND ABUNDANCIES IN PRESENCE OF PHASE SEPARATION

In this section, we carry out an MC study of layer occupancies in the FCSOS model, now under strict *canonical*, particle-conserving conditions. We do this to see whether the phase-separation scenario earlier introduced is confirmed, and if so what are the implications for a realistic canonical situation, such as that of a standard MD simulation, or of a suitably fast experiment on a step-free metal surface.

We choose convenient, but otherwise arbitrary, Hamiltonian parameters and temperature, namely, $J=0$ and $e^{\beta K}=e^{\beta L}=5$. Here, Hamiltonian (8) is known to give rise to a DOF phase.¹⁹ We start with a full layer, i.e., $M=0$ in magnetic language. Canonical MC moves are of the Kawasaki type, which conserves \bar{h} . They consist of choosing pairs of lattice sites i and j some distance l_{ij} apart, and then updating heights $h_i \rightarrow h_i - 3$ and $h_j \rightarrow h_j + 3$, as if a particle jumped from i to j . In our case l_{ij} includes up to fourth neighbors in the triangular lattice. Moves are always accepted in accordance with detailed balance.

After a short transient, about 3 000 000 MC sweeps are generated at equilibrium. Over this trajectory in phase space, we evaluate the abundance and occupancy of each surface layer. This is done for increasing linear sizes, namely, $N = \sqrt{N_i} = 24, 36, 48, 60, 72$. The results are then plotted to check the form $\ln[a_n^{\infty} - a_n(N)] = \ln C_n + \ln N$, suggested by Eq. (8). This form is in fact used as a fitting form, with a_n^{∞} and C_n as parameters.

Figure 2 shows the fitting details for the topmost (adatom) layer 1. The fit is quite good, yielding $a_{\text{top}}^{\infty} = \frac{1}{12} \pm 0.003$ and $C_{\text{top}} \approx 0.365$. For the first surface layer (layer 0), we similarly found the expected abundance of $\frac{1}{4}$ with exactly the same finite-size behavior as that of adatoms in Fig. 2. On the other hand, the abundance of the second layer below adatoms, layer -1 , deviates progressively from $\frac{1}{3}$, as N grows, as shown in Fig. 3. This is physically reasonable, reflecting, as required by sum rule (2), the presence of a small but

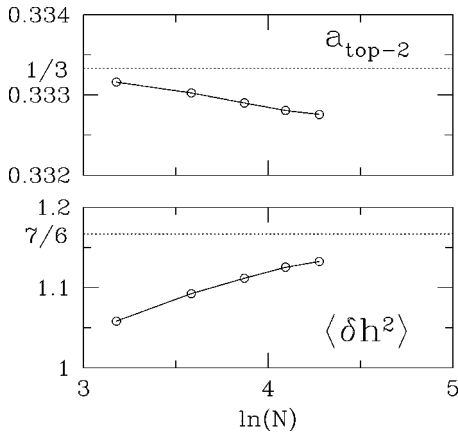


FIG. 3. FCSOS model with full layers: above, scaling of abundance of layer -1 as a function of the lattice size. This quantity appears to saturate at a value slightly smaller than $\frac{1}{3}$ (see text); below, scaling of the average square height difference as a function of the lattice size. In an ideal DOF-separated surface, this quantity must be equal to $\frac{7}{6}$.

finite number of “ad-adatoms” in the second adlayer, layer 2. Similar evidence of T -dependent deviations from the ideal abundancy map was also found in the DOF phase, as obtained in Ref. 4 by grand-canonical MC simulation. They account for the small but nonzero deviation of $\langle \delta h^2 \rangle$ from $\frac{11}{12}$, visible in their Fig. 8 (similarly, in the canonical simulation $\langle \delta h^2 \rangle$ tends to approximately $\frac{7}{6}$; see Fig. 3 below). We note here that SOS models are artificially asymmetric in that they permit adatoms, but forbid buried vacancies. The artificial absence of deep vacancies appears to be the main reason why abundancies in layers 1 and 0 scale very accurately to $\frac{1}{2}$ and $\frac{1}{4}$. Deviations would, of course, be expected in a more realistic description.

We cannot at this stage rule out deviations from the scaling behavior (8) which could arise if, for example, some microscopic length scale were to enter the problem; in any case, we have found no evidence of them. We therefore conclude that the expected macroscopic phase separation of a flat integer-layer surface into two half-integer DOF domains is confirmed. Although obtained at a single point in the phase diagram, it is reasonable to assume that this behavior is generic, and applicable for different temperatures or even different Hamiltonians, so long as one stays inside the DOF phase.

V. DOF PHASE SEPARATION IN PARTICLE-CONSERVING MD SIMULATIONS

Preroughening-related phenomena have been proposed earlier for metal surfaces, in particular fcc(110) noble metal faces.^{2,3,6,7} In spite of some experimental suggestions in this direction,^{20,21} there is as yet no clear consensus about their existence on real surfaces. One might even suspect that restricted SOS models lack some fundamental ingredient, which makes real surfaces different. A useful step is therefore to consider whether PR and DOF phases are or are not present in *realistic* simulations of metal surfaces. Particle-conserving, off-lattice MD simulations, with continuous coordinates and realistic interparticle potentials, have been very popular for crystal surfaces. Lennard-Jones surfaces and their

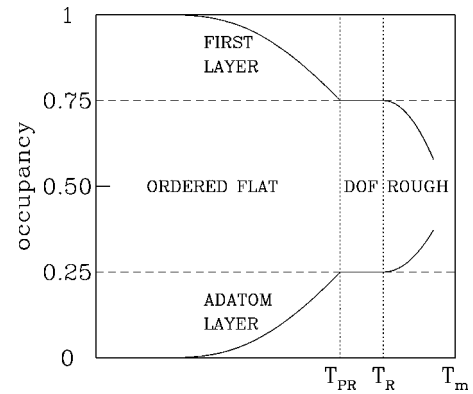


FIG. 4. Schematic behavior of occupancies of the first two layers of an initially full-layered surface as a function of temperature. A characteristic plateau between preroughening and roughening is expected, indicating phase separation into DOF domains.

thermal disordering have been extensively investigated for over two decades.²² Since the advent of quantitatively constructed, even if empirical or semiempirical, many-body potentials, metal surfaces have also been widely studied in this manner. Simulation evidence has been reported or construed about a variety of phase transitions—among them reconstruction, deconstruction, roughening, surface melting, faceting, etc.⁹ However, no evidence or claim of PR (or the lack of it) is usually advanced based on this kind of simulation results.²³ The main difficulty in trying to do that is precisely because of the fixed particle number, most often full layers, involved in the simulation.

However, the mechanism just described of phase separation into DOF domains separated by monatomic steps, should be at work in these simulations too. The scope of this section is to reexamine some of the existing metal surface simulations, searching for possible evidence of a previously unnoticed DOF phase separation. In particular, we concentrate on layer occupancies, a quantity particularly easy to extract from realistic simulations, and therefore often available. Our qualitative expectations are summarized in Fig. 4 for an initial full layer at $T=0$. At low temperatures, the number of first-layer vacancies and of adatoms is expected—in thermal equilibrium—to be very small, growing in an Arrhenius-like fashion with temperature. On surfaces such as metal fcc(110), eventually undergoing roughening and surface melting close to T_m , this adatom/vacancy concentration is known to grow very substantially with T , reaching values as high as 0.1 already at $T \approx 0.6T_m$ (T_m is the bulk melting temperature).²⁴ It was actually pointed out, some time ago, that proliferation of surface vacancies and/or adatoms is one of the earliest precursors of surface melting.^{24,25}

Our basic expectation is that the particle-conserving simulated metal surface will phase separate into two coexisting DOF phases, as soon as $T=T_{PR}$ is reached. Since the DOF phase remains stable up to $T=T_R$, the occupancies of the first layer and of the adatom layer should be pinned at $\frac{3}{4}$ and $\frac{1}{4}$, from PR until roughening. Hence, if the lattice model predictions hold in a realistic case, PR should be signaled by the onset of a characteristic plateau—due to phase separation—of the first-layer vacancy and adatom concentrations. In other words, at $T=T_{PR}$ the previously activated

growth of the surface vacancy and adatom concentrations should suddenly pause, and not restart again until roughening is reached at $T=T_R$. We can now examine in this light some existing metal surface simulations, in particular those of the (110) surfaces, where disordering is more pronounced.

(i) Al(110). The full-layer canonical MC and MD simulations by van der Gon *et al.* indicate that the first-layer occupancy decreases steadily from 1 to ≈ 0.85 at the bulk melting point of Al. Another more recent and detailed MD simulation of Al(110) in our group⁹ similarly yields $o_0=0.82, 0.85$, and 0.82 at $T/T_m=0.946, 0.973$, and 0.989 , respectively, but also corresponding adatom occupancies $o_1=0.22, 0.25$, and 0.28 . Hence adatoms display an approximate plateau at occupancy $1/4$. Vacancies also have a plateau, even if somewhat below the $\frac{1}{4}$ occupancy. While this kind of evidence perhaps cannot be considered conclusive, it is certainly very suggestive of a DOF phase separation. The smaller concentration of surface first-layer vacancies (between 0.15 and 0.18 instead of $1/4$) appears mostly related to the presence of deep vacancies, which are absent in SOS models. As also shown by other MD simulations for metals, close to the melting point buried vacancies spread very substantially inwards to layers deeper than the first, while adatoms spread outwards much less. For instance, the above occupancies imply that on Al(110) at $0.95T_m$ the deep vacancies are as many as 10% of a monolayer. At the moment, it is not clear if the deep vacancies could partly represent an artifact associated with the phase separation, or whether they are real, and would therefore persist under fully grand-canonical conditions. This question remains open.

(ii) Pb(110). Full-layer simulations of this surface with a ‘‘glue’’ model forces have been published in Ref. 26. There are clear signs of surface mobility at $400\text{ K}\approx\frac{2}{3}T_m$ ($T_m=619\pm 5\text{ K}$ for this potential²⁷). However, the layer occupancies were not provided by these authors. Experimentally, antiphase scattering anomalies have been reported around 340 K ,²¹ which might correspond to T_{PR} for this surface. This temperature is very low, but it is not incompatible with the known $T_R\approx 415\text{ K}$ for Pb(110).²¹ A more detailed analysis of simulation results as well as fresh experiments, are thus called for also in this case.

(iii) Ni(110). den Nijs³ suggested that scattering data by Cao and Conrad²⁰ support PR of this surface at $T\approx 1300\text{ K}$, while roughening does not take place until $\approx 1400\text{ K}$. An early simulation in Ref. 28, on the other hand, suggests a nonzero population of adatoms only at 1450 K . Subsequently, in that simulation, the adatom occupancy grows with temperature, reaching 0.25 only some 30 degrees below their embedded-atom-method model potential’s melting point, $T_m=1733\text{ K}$, without much of a plateau, at least with the relatively small sizes used (70 atoms/layer). Larger size simulations would be necessary in this case, as well as a critical assessment of the quality of the description provided for Ni(110) by this potential, since the results appear to be inconsistent with Cao and Conrad’s data.

(iv) Cu(110). Old data by Stock and Menzel²⁹ indicate that this surface roughens well below T_m . A recent MC/MD simulation by Merikoski *et al.*³⁰ suggested $T_R\approx 1000\text{ K}$. Their full-layer large-size MD simulation at $T=1150\text{ K}$, in particular, found occupancies $o_{-1}=0.96$, $o_0=0.77$,

$o_1=0.25$, and $o_2=0.025$. The closeness of these o_0 and o_1 values to the phase-separated DOF values $\frac{3}{4}$ and $\frac{1}{4}$ is striking. This suggests, interestingly, that the plateau occupancies $3/4$ and $1/4$ typical of DOF phase separation not only show up very clearly, but also that they may persist even above T_R , at least under the conditions of finite terrace size corresponding to this simulation. It should be interesting to pursue the possibility of PR of this surface experimentally.

VI. CONCLUSIONS

In this paper, we have considered the phase separation of a particle-conserving (‘‘canonical’’) full-layered metal surface into disordered flat (DOF) domains of opposite order parameter, each domain having a half-full layer on top. The phase separation has been demonstrated microscopically by a Gibbs-ensemble calculation on a lattice Hamiltonian model. A fully canonical MC study of layer occupancies, conducted with finite-size scaling in order to reduce progressively the importance of the interface between the two phases, gives further strength to the phase-separation picture.

A number of published particle-conserving realistic MD simulations for fcc(110) metal surfaces have been analyzed in this light. It is argued that at least some of them display clear, previously unrecognized evidence of a DOF phase separation. The main signal of that is a plateau of layer occupancies with temperature, around values close to $\frac{3}{4}$ for the first crystal layer, and around $\frac{1}{4}$ for the adatom layer.

In all cases where DOF phase separation is proven, or even only suspected, one should reconsider the results of canonical simulations with new eyes. In fact these simulations will not automatically represent the experimental reality, unless the experiment is very specially designed, with very short times and very large terraces. In all other cases, which means a vast majority of all presently available data, the true state of affairs, corresponding to a well-defined single-domain DOF surface, could only be compared with a yet-to-come realistic *grand-canonical* simulation. We are currently developing such a scheme in our group.

On the experimental side, time-resolved fast surface heating experiments could be used on very flat, step-free surfaces, as a tool to uncover a DOF phase separation on candidate metal surfaces, such as Pb(110) or Cu(110).

ACKNOWLEDGMENTS

We are very grateful to F. Di Tolla, F. Ercolessi, C. S. Jayanthi, and G. Santoro for discussions and information, including access to their unpublished results. One of us (S.P.) wishes to thank SISSA for hospitality. This research was supported in part by the Consiglio Nazionale delle Ricerche (CNR) under the ‘‘Progetto Finalizzato ‘Sistemi informatici e calcolo parallelo’,’’ by EEC under Contracts No. ERBCHRXCT 930342 and No. ERBCHBGCT 940636, and by INFN under PRA LOTUS.

APPENDIX

In this appendix we derive an expression for the chemical potential in general SOS systems (including restricted ones) in terms of the average Boltzmann weight for the insertion of a new particle. We do this both in the canonical and in the

Gibbs ensemble. This result generalizes to SOS systems the standard Widom expression for continuous simple fluids.¹⁷ Moreover, we explain how to implement our formula in a MC calculation.

The partition function of the SOS model at fixed \bar{h} reads

$$Z_{\bar{h},N_t}(\beta) = \sum_{\{h\}}^{(\bar{h})} e^{-\beta E\{h\}}, \quad (\text{A1})$$

where the sum is over height configurations (of energy $E\{h\}$) such that $\sum_i h_i = N_t \bar{h}$.

Inserting one particle into the surface changes the mean height by a factor $1/N_t$, and the partition function becomes

$$Z_{\bar{h}+(1/N_t),N_t}(\beta) = \sum_{\{h\}}^{[\bar{h}+(1/N_t)]} e^{-\beta E\{h\}} = \sum_{\{h\}}^{(\bar{h})} \frac{1}{N_t} \sum_{i=1}^{N_t} e^{-\beta E\{h\}_i^+}, \quad (\text{A2})$$

where $\{h\}_i^+$ has an extra particle at site i , and $1/N_t$ avoids multiple counting.

Now we multiply and simultaneously divide by $e^{-\beta E\{h\}}$, obtaining

$$Z_{\bar{h}+(1/N_t),N_t}(\beta) = Z_{\bar{h},N_t}(\beta) \left\langle \frac{1}{N_t} \sum_{i=1}^{N_t} e^{-\beta \Delta E_i^+} \right\rangle, \quad (\text{A3})$$

where $\Delta E_i^+ = E\{h\}_i^+ - E\{h\}$ and the average is over the constant \bar{h} ensemble. Finally, the chemical potential is

$$\begin{aligned} \beta\mu &= -\frac{k_B T}{N_t} \left(\frac{\partial \ln Z_{\bar{h}}}{\partial \bar{h}} \right) = -k_B T \ln \frac{Z_{\bar{h}+(1/N_t),N_t}(\beta)}{Z_{\bar{h},N_t}(\beta)} \\ &= -k_B T \ln \left\langle \frac{1}{N_t} \sum_{i=1}^{N_t} e^{-\beta \Delta E_i^+} \right\rangle. \end{aligned} \quad (\text{A4})$$

By analogy with the hard-sphere system, the average in Eq. (A4) can be viewed as a sort of ‘‘insertion probability.’’ The best way to calculate this quantity in a MC calculation is to alternate attempted insertions of an extra particle to standard particle-conserving Kawasaki moves. During an insertion trial move, a height chosen at random is incremented and the factor $e^{-\beta \Delta E}$ is evaluated (in case of a restricted SOS model, this factor is zero if the move does not fit the constraints). In

any case, the particle that has been added is then removed. At the end, all those factors $e^{-\beta \Delta E}$ are summed and the sum is divided by the number of trial insertions.

In the Gibbs ensemble, we consider first the expression for the partition function,

$$Z_{\bar{h},2N_t}^{\text{GIBBS}}(\beta) = \int_{-\infty}^{+\infty} d\Delta Z_{\bar{h}+\Delta,N_t}(\beta) Z_{\bar{h}-\Delta,N_t}(\beta), \quad (\text{A5})$$

in terms of the canonical partition functions of the surfaces in the two $\sqrt{N_t} \times \sqrt{N_t}$ boxes at fixed mean heights $\bar{h}_1 = \bar{h} + \Delta$ and $\bar{h}_2 = \bar{h} - \Delta$, respectively.

Now observe that it is possible to increment the total mean height by $1/2N_t$ (i.e., to add a particle) in two equivalent ways, namely, by inserting one particle either into box 1 or into box 2. Thus

$$\begin{aligned} Z_{\bar{h}+(1/2N_t),2N_t}^{\text{GIBBS}}(\beta) &= \frac{1}{2} \int_{-\infty}^{+\infty} d\Delta Z_{\bar{h}+(1/2N_t)+\Delta,N_t}(\beta) Z_{\bar{h}-\Delta,N_t}(\beta) \\ &\quad + \frac{1}{2} \int_{-\infty}^{+\infty} d\Delta Z_{\bar{h}+\Delta,N_t}(\beta) Z_{\bar{h}+(1/2N_t)-\Delta,N_t}(\beta) \\ &= \frac{1}{2} Z_{\bar{h},2N_t}^{\text{GIBBS}}(\beta) \sum_{\alpha=1,2} \left\langle \frac{1}{N_t} \sum_{i=1}^{N_t} e^{-\beta \Delta E_i^+} \right\rangle_{\alpha}, \end{aligned} \quad (\text{A6})$$

which finally gives μ as

$$\mu = -k_B T \ln \left\{ \frac{1}{2} \sum_{\alpha=1,2} \left\langle \frac{1}{N_t} \sum_{i=1}^{N_t} e^{-\beta \Delta E_i^+} \right\rangle_{\alpha} \right\}. \quad (\text{A7})$$

It is important to stress that the average $\langle \dots \rangle_{\alpha}$ is now a Gibbs-ensemble average. Looking at Eq. (A7), it is not strictly possible, as also observed in Ref. 18, to calculate the chemical potential of the two subsystems separately. However, if the two phases maintain their own identities during the MC run, and the two averages are identical, then we can conclude that the chemical potential of each box is properly defined and is the same for both. Finally, observe that, as noticed in Ref. 11, we can obtain the test particle interaction energies in the course of the attempted exchange steps, without inclusion of extra test particles. This avoids supplementary insertion moves and speeds up the calculation.

*Electronic address: prestip@agave.unime.it

†Electronic address: tosatti@sissa.it

¹M. den Nijs and K. Rommelse, Phys. Rev. B **40**, 4709 (1989).

²G. Mazzeo, G. Jug, A. C. Levi, and E. Tosatti, Surf. Sci. **273**, 237 (1992); Europhys. Lett. **22**, 39 (1993); Phys. Rev. B **49**, 7625 (1994).

³M. den Nijs, in *Phase Transitions in Surface Films*, edited by H. Taub *et al.* (Plenum, New York, 1991), Vol. 2.

⁴S. Prestipino, G. Santoro, and E. Tosatti, Phys. Rev. Lett. **75**, 4468 (1995).

⁵V. I. Marchenko and A. Ya. Parshin, Zh. Éksp. Teor. Fiz. **79**, 257 (1980) [Sov. Phys. JETP **52**, 129 (1980)]; P. Nozières, in *Solids Far From Equilibrium*, edited by C. Godrèche (Cambridge University Press, Cambridge, 1992).

⁶G. Jug and E. Tosatti, Phys. Rev. B **42**, 969 (1990); Physica A

175, 59 (1991); J. Kohanoff, G. Jug, and E. Tosatti, J. Phys. A **23**, L209 (1990); **23**, 5625 (1990).

⁷M. den Nijs, Phys. Rev. B **46**, 10 386 (1992).

⁸G. Santoro, M. Vendruscolo, S. Prestipino, and E. Tosatti, Phys. Rev. B **53**, 13 169 (1996); G. Santoro and M. Fabrizio, *ibid.* **49**, 13 886 (1994).

⁹F. D. Di Tolla, E. Tosatti, and F. Ercolessi, in *Monte Carlo and Molecular Dynamics of Condensed Matter Systems*, edited by K. Binder and G. Ciccotti (SIF, Bologna, 1996), Vol. 49, p. 345; F. D. Di Tolla, Ph.D. thesis, SISSA, Trieste, 1995; and (private communication).

¹⁰M. P. Allen and D. J. Tildesley, *Computer Simulation of Liquids* (Clarendon, Oxford, 1987).

¹¹A. Z. Panagiotopoulos, Mol. Phys. **61**, 813 (1987); A. Z. Panagiotopoulos, N. Quirke, M. Stapleton, and D. Tildesley, *ibid.* **63**, 527 (1988).

- ¹²J. I. Siepmann, S. Karaborni, and B. Smit, *Nature (London)* **365**, 330 (1993); B. Smit, S. Karaborni, and J. I. Siepmann, *J. Chem. Phys.* **102**, 2126 (1995).
- ¹³A. Z. Panagiotopoulos, *Mol. Simul.* **9**, 1 (1992).
- ¹⁴B. Smit, P. de Smedt, and D. Frenkel, *Mol. Phys.* **68**, 931 (1989).
- ¹⁵K. K. Mon and K. Binder, *J. Chem. Phys.* **96**, 6989 (1992).
- ¹⁶S. Prestipino and E. Tosatti (unpublished).
- ¹⁷B. Widom, *J. Chem. Phys.* **39**, 2808 (1963).
- ¹⁸B. Smit and D. Frenkel, *Mol. Phys.* **68**, 951 (1989).
- ¹⁹Since here we have no Glauber-type, particle creation or destruction moves, values of K and L which are not too large are preferable, in order to have reasonable acceptances for the farthest Kawasaki-type, particle-conserving moves.
- ²⁰Y. Cao and E. H. Conrad, *Phys. Rev. Lett.* **64**, 447 (1990).
- ²¹H. N. Yang, K. Fang, G.-C. Wang, and T.-M. Lu, *Europhys. Lett.* **19**, 215 (1992).
- ²²J. Q. Broughton and L. V. Woodcock, *J. Phys. C* **11**, 2743 (1978); J. Q. Broughton and G. H. Gilmer, *J. Chem. Phys.* **79**, 5105 (1983); **79**, 5119 (1983).
- ²³A notable exception is an *ab initio* simulation of Ge(111), where preroughening has been suggested to take place in correspondence with melting and metallization of the first bilayer. See N. Takeuchi, A. Selloni, and E. Tosatti, *Phys. Rev. Lett.* **72**, 2227 (1994).
- ²⁴A. W. Denier van der Gon, D. Frenkel, J. M. W. Frenken, R. J. Smith, and P. Stoltze, *Surf. Sci.* **256**, 385 (1991).
- ²⁵P. Stoltze, J. K. Norskov, and U. Landman, *Surf. Sci.* **220**, L693 (1989).
- ²⁶C. P. Toh, C. K. Ong, and F. Ercolessi, *Phys. Rev. B* **50**, 17 507 (1994).
- ²⁷A. Landa, P. Wynblatt, H. Häkkinen, R. N. Barnett, and U. Landman, *Phys. Rev. B* **51**, 10972 (1995).
- ²⁸E. T. Chen, R. N. Barnett, and U. Landman, *Phys. Rev. B* **40**, 924 (1989); **41**, 439 (1990).
- ²⁹K. D. Stock and E. Menzel, *Surf. Sci.* **61**, 272 (1976); *J. Cryst. Growth* **43**, 135 (1978); K. D. Stock, *Surf. Sci.* **91**, 655 (1980).
- ³⁰H. Häkkinen, J. Merikoski, M. Manninen, J. Timonen, and K. Kaski, *Phys. Rev. Lett.* **70**, 2451 (1993); J. Merikoski, H. Häkkinen, M. Manninen, J. Timonen, and K. Kaski, *Phys. Rev. B* **49**, 4938 (1994).